Polymer Bulletin 49, 197-203 (2002)

Polymer Bulletin

Study of the amorphous phase in semicrystalline poly(ethylene terephthalate) via dynamic mechanical thermal analysis

Wei Dong[1,2], Jun Zhao[1], Chaoxu Li[1], Meili Guo[2], Delu Zhao[1], Qingrong Fan[1] (✉)

[1]State Key Laboratory of Polymer Physics & Chemistry, Center for Molecular Science, Institute of Chemistry, Chinese Academy of Sciences, Beijing 100080, P. R. China
[2]College of Materials Science and Engineering, Beijing University of Aeronautics and Astronautics, Beijing 100083, P. R. China
e-mail: qrfan@pplas.icas.ac.cn, Tel.: +86-10-62563065, Fax: +86-10-62559373

Received: 22 July 2002/Revised version: 19 September 2002/ Accepted: 23 September 2002

Summary

Characters of amorphous phase in semicrystalline poly(ethylene terephthalate) (PET) were investigated systematically via dynamic mechanical thermal analysis (DMTA) in this paper. It was found that the storage modulus (E') and the glass transition temperature (T_g) of semicrystalline PET changed with the degree of crystallinity (X_c). T_g showed good linearity with X_c. However, neither reduction of E' in the T_g region (ΔlgE') nor loss tangent (tanδ) at the T_g presented linearity with X_c, which suggests that the two-phase model was not suitable for semicrystalline PET. It was also confirmed that the physical aging reduced the chain segmental mobility, producing higher T_g.

Introduction

Poly(ethylene terephthalate) (PET) is one of the most commercially important polyesters. It finds widespread uses in fibers, films, and other engineering components [1,2]. There have been many reports about the investigations on its morphology of crystalline phase [3-5], but less attention was paid to its amorphous phase and many aspects have not yet been fully clarified [6,7].

This paper constitutes the third piece of a series of papers relative to the study of amorphous phase in semicrystalline PET. In our previous papers [8,9], we had reported that when the degree of crystallinity (X_c) was within a definite range, there were dual amorphous phases with quite different chain segmental mobility: free amorphous phase with higher mobility and constrained amorphous phase with lower mobility. The dual amorphous phases could show as dual loss tangent (tan δ) peaks at α transition region in dynamic mechanical thermal analysis (DMTA) curves. And when the semicrystalline samples had been physically aged, there were dual endothermic physical aging peaks appearing in the glass transition region of differential scanning calorimetric (DSC) traces. The conditions under which the dual amorphous phases coexisted and their mutual transition laws during the physical aging were also discussed [8,9].

In our further study, we found that the overlapping of dual tan δ peaks was unavoidable due to the fact that the width of the lower tan δ peak was ca. 20 – 30 °C and that of the upper peak ca. 40 - 60 °C, whereas the difference between their peak temperatures was only ca. 15 °C. As a result, in most cases, only the dominant single peak could be observed [10].

In this paper, changes of amorphous phase in semicrystalline PET during isothermal crystallization and physical aging will be further studied mainly by means of DMTA, which is more sensitive than DSC to the glass transition and other secondary transition in polymers [11-13].

Experimental

Samples preparation

Amorphous PET films were kindly supplied by Beijing Plastics Co. The samples had a thickness of ca. 0.15 mm, a viscosity-average molecular weight of ca. 1.63×10^4, a density of ca. 1.335 g cm^{-3} which means that samples were wholly amorphous, and an optical birefringence of ca. 6×10^{-4} which means that there was no orientation. Measurements by both DSC and wide-angle X-ray diffraction (WAXD) also showed that the samples were wholly amorphous.

Thermal treatments

As-received PET films were cut into equal rectangles with a size of ca. 20.0×5.0 mm^2. They were held in an oven in nitrogen atmosphere at 300 ± 0.5 °C (ca. 45 °C above their melting temperature (T_m) of ca. 255 °C) for 5 min to completely eliminate their thermal history. Then these samples were quenched in air to room temperature of ca. 25 °C. It has proved that there was no crystallization induced by this process. Subsequently, these quenched samples crystallized isothermally in an oven in nitrogen atmosphere at 130 °C for different time to obtain different X_c. Ten samples were prepared for each crystallization time, and five of them were physically aged in an oven in nitrogen atmosphere at 68 °C for seven days. Finally, all these physically aged and unaged semicrystalline samples were taken out for DMTA measurements.

DMTA measurments

DMTA measurements were performed in a Rheometric Scientific DMTA □ at a frequency of 1 Hz and a heating rate of 5 °C min^{-1} by tension mode. Samples were stretched by a constant stress of 0.2 N. The temperature range of measurements was from room temperature to 160 °C. Curves of dynamic modulus ($E^* = E' + iE''$) and tanδ ($= E'' / E'$) vs temperature were obtained, respectively.

X_c measurements

X_c of semicrystalline PET was measured by using a TA2910 DSC. Indium and tin were employed for the temperature calibration, and the specific heat capacity was evaluated with respect to sapphire as a standard. The mass of samples was ca. 3.0 mg and a nitrogen gas purge with a flux of ca. 20 mL min^{-1} was used to prevent oxidative degradation of samples during the heating run. The rate of heating run in DSC was 30 °C min^{-1}. X_c was calculated by the following equation [1]:

$$X_c\,(\%) = (35.10 - \Delta H_{cc}) \times 100 / 135.8 \qquad \textbf{(1)}$$

in which 35.10 J g^{-1} was the cold crystallization enthalpy (ΔH_{cc}) of wholly amorphous PET and 135.8 J g^{-1} was the melting enthalpy of perfect crystalline lamellae [1].

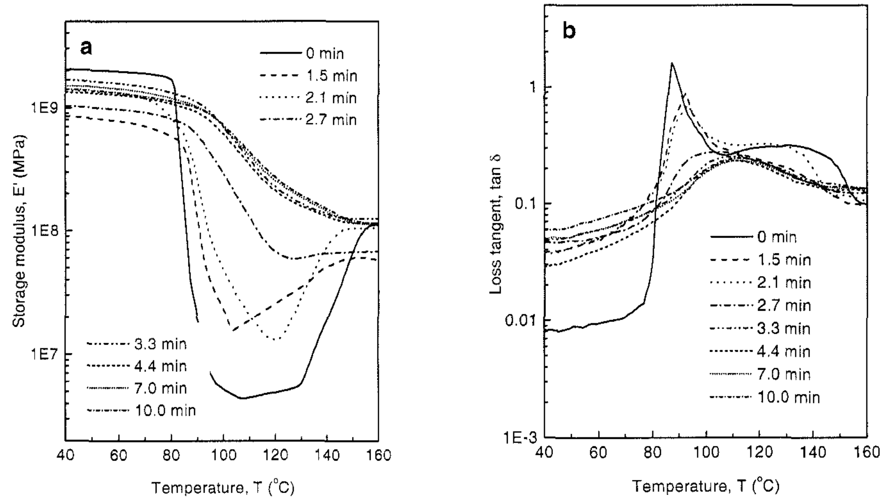

Figure 1 DMTA curves of semicrystalline PET crystallized isothermally at 130 °C for different t_c indicated in the corner: E' (a), tan δ (b).

Results and discussion

Figure 1 presents DMTA traces of semicrystalline PET crystallized isothermally at 130 °C for different time. It can be seen that the shape of curves changed greatly with change of crystallization time (t_c). Thus, different characters of amorphous phase in semicrystalline samples can be obtained from these curves.

As shown in Figure 1a, when t_c was above 3.3 min, there was only a step with a width of over 70 °C appearing in the T_g region of storage modulus (E') curves of semicrystalline samples. However, when t_c was below 2.1 min, an obvious E' peak could be found at temperatures above but close to the T_g. This E' peak could be attributed to the cold crystallization of semicrystalline samples with a low X_c [14,15]. When t_c was between these two cases, a transition case could be seen where the cold crystallization peak disappeared gradually.

From Figure 1b, it can be seen that when t_c was above 3.3 min, there was only a smooth α transition peak with a width of ca. 60 °C appearing in the glass transition region of tan δ curves of semicrystalline samples. However, when t_c was below 2.1 min, an obvious plateau with a width of ca. 45 °C could be found at higher temperatures besides a sharp α transition peak with a width of ca. 30 °C in the glass transition region. This tan δ peak could also be attributed to the cold crystallization of semicrystalline samples with a low X_c [14.15]. When t_c was between these two cases, a transition case could also be seen where the cold crystallization plateau disappeared gradually.

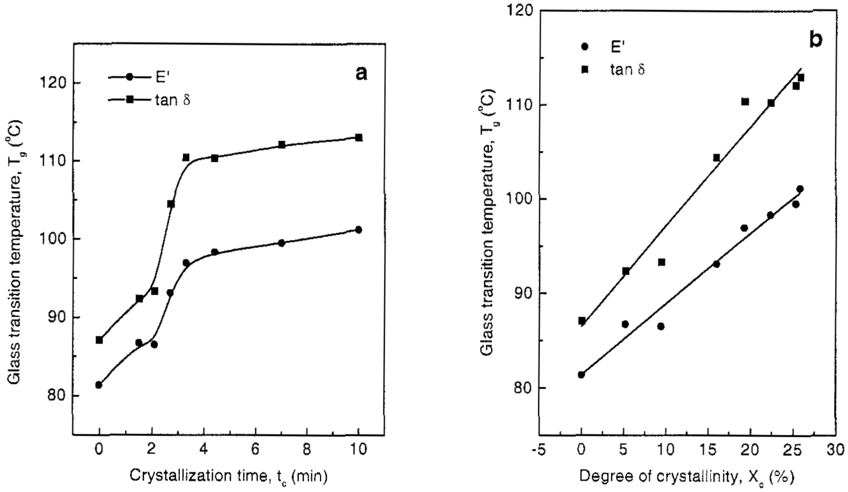

Figure 2 Evolution of T_g measured by two different methods indicated in the corner with increasing t_c (a) and X_c (b) (measured from Figure 1).

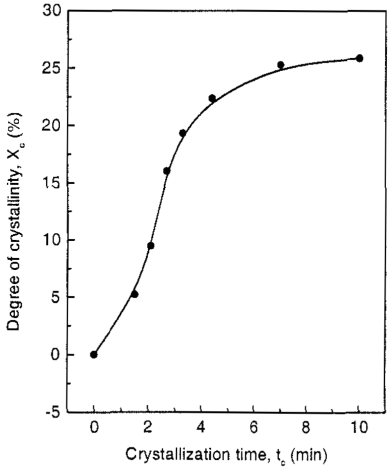

Figure 3 Evolution of X_c with increasing t_c for PET crystallized isothermally at 130 °C.

In DMTA measurements, both inflexion of step in the glass transition region of E' curves and peak temperature of α transition peaks in tan δ curves can be employed as the T_g. Figure 2 presents the change laws of T_g with increasing t_c and X_c, where T_g was measured by these two methods, respectively. It can be seen that T_g shifted to higher temperatures continuously with increasing t_c or X_c, which is consistent with others' report [12,15]. The increase of T_g with increasing t_c showed a sigmoid shape where rapid increase occurred at ca. 2.1 - 3.3 min, while a good linearity could be seen for the increase of T_g with increasing X_c.

Figure 3 showed the isothermal crystallization kinetics of PET at 130 °C measured by DSC. It can be seen that the increase of X_c also showed sigmoid shape with increasing t_c. The t_c range where rapid increase of X_c occurred was ca. 1.5 - 4.4 min, which was a little wider than the t_c range shown in Figure 2a.

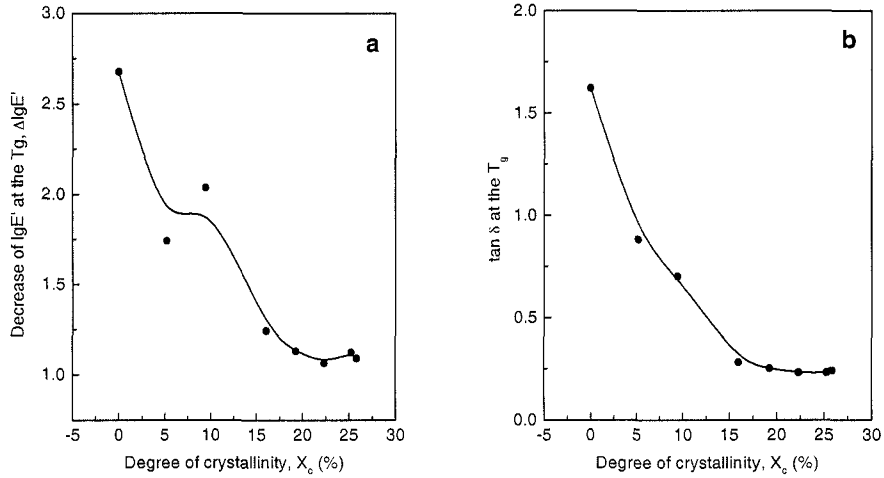

Figure 4 Evolution of ΔlgE' (a) and tan δ at the T_g (b) with increasing X_c (measured from Figures 1 and 3).

Figure 4 presents change laws of the heights of E' steps (i.e. the decreases of E' in the T_g region, ΔlgE') and the α transition peak values in tan δ curves (i.e. tan δ at the T_g) with increasing X_c, respectively. It can be seen that both ΔlgE' and tan δ at the T_g decreased rapidly with increasing X_c for the low X_c, and when X_c reached a relatively high value both ΔlgE' and tan δ at the T_g remained constant.

Some literature ever reported the following empirical equation on the basis of two-phase model of semicrystalline polymers [16]:

$$\tan\delta \ \square\ X_c \tan \delta_c \ \square\ (1 - X_c) \tan \delta_a \qquad (2)$$

where $\tan \delta_c$ and $\tan \delta_a$ represented the contribution of crystalline phase and amorphous phase to tan δ, respectively. Equation (2) can also be written as the following equation (3):

$$\tan\delta \ \square\ (\tan \delta_c - \tan \delta_a) X_c \ \square\ \tan \delta_a \qquad (3)$$

If the two-phase model worked in the semicrystalline PET, tanδ should show good linearity with X_c, and the slope and the intercept be $(\tan \delta_c - \tan \delta_a)$ and $\tan \delta_a$, respectively.

Clearly, our experimental results didn't consist with these two empirical equations, which suggests that the semicrystalline PET couldn't be described by the two-phase model. In fact, the three-phase and even multiphase model has proved to be more suitable for semicrystalline PET [8,9].

Figure 5 presents influence of the physical aging on DMTA properties of semicrystalline PET. From Figure 5a, it can be seen that, with the proceeding of physical aging, α transition peak in DMTA curves shifted to higher temperatures while tan δ value decreased for both samples. The former law can be seen more clearly in Figure 5b, where more semicrystalline samples with various X_c were measured. These results showed that physical aging did reduce the chain segmental mobility of semicrystalline samples. In the literature, no such results could be clearly observed because no appropriate physical aging conditions were used [13,17].

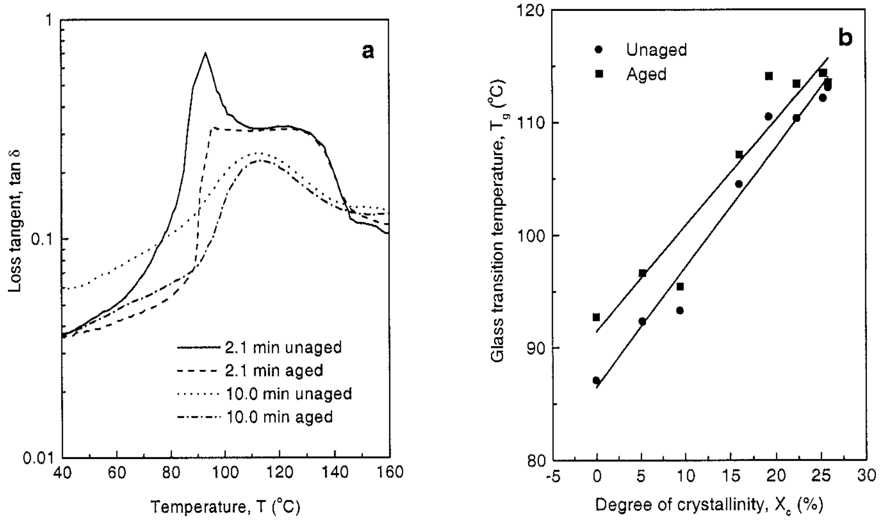

Figure 5 Effect of physical aging on the DMTA curves of semicrystalline PET (a) and their T_g (b).

In conclusion, our systematical investigations showed that E' and T_g of semicrystalline PET changed with X_c. T_g presented good linearity with X_c, but ΔlgE' and tan δ at T_g didn't present linearity with X_c, which indicates that the two-phase model didn't fit semicrystalline PET. Besides, constraint of the physical aging on the mobility of molecular segments was confirmed.

Acknowledgements.

This work was subsidized by the Special Funds for Major State Basic Research Projects (95-12 and G1999064800).

References

1. Jog JP (1995) J Macromol Sci Rev Macromol Chem Phys C35:531.
2. Schmidt-Rohr K, Hu W, Zumbulyadis N (1998) Science 280:714.
3. Santa-Cruz C, Stribeck N, Zachmann HG, Baltá-Calleja FJ (1991) Macromolecules 24:5980.
4. Rule RJ, MacKerron DH, Mahendrasingam A, Martin C, Nye TMW (1995) Macromolecules 28:8517.
5. Sakai Y, Imai M, Kaji K, Tsuji M (1996) Macromolecules 29:8830.
6. Bove L, D'Aniello C, Gorrasi G, Guadagno L, Vittoria V (1997) Polym Bull 38:579.
7. McGonigle EA, Daly JH, Gallagher S, Jenkins SD, Liggat JJ, Olsson I, Pethrick RA (1999) Polymer 40:4977.

8. Zhao J, Song R, Zhang Z, Linghu X, Zheng Z, Fan Q (2001) Macromolecules 34:343.
9. Zhao J, Wang J, Li C, Fan Q (2002) Macromolecules 35:3097.
10. Groeninckx G, Berghmans H, Smets G (1976) J Polym Sci 14:591.
11. Alice Ng CW, MacKnight WJ (1996) Macromolecules 29:2412.
12. Hay JN (1995) Pure Appl Chem 67:1855.
13. Siegmann A, Turi E (1974) J Macromol Sci Phys B10:689.
14. Aoki Y, Li L, Amari T, Nishimura K, Arashiro Y (1999) Macromolecules 32:1923.
15. Chen M, Hellgeth JW, Siochi EJ, Ward TC, Mcgrath JE (1993) Polym Eng Sci 33:1122.
16. Gray RW, McCrum NG (1969) J Polym Sci A2:1329.
17. Vigier G, Tatibouet J (1993) Polymer 34:4257.